



Efficient Light-Driven Hydrogen Evolution Using a Thiosemicarbazone-Nickel (II) Complex

Stylianos Panagiotakis¹, Georgios Landrou¹, Vasilis Nikolaou¹, Anisa Putri², Renaud Hardré², Julien Massin², Georgios Charalambidis^{1*}, Athanassios G. Coutsolelos^{1*} and Maylis Orio^{2*}

¹Laboratory of Bioinorganic Chemistry, Department of Chemistry, University of Crete, Heraklion, Greece, ²Aix Marseille Université, CNRS, Centrale Marseille, iSm2, Marseille, France

OPEN ACCESS

Edited by:

Bunsho Ohtani,
Hokkaido University, Japan

Reviewed by:

Marco Armandi,
Polytechnic University of Turin, Italy
Mirco Natali,
University of Ferrara, Italy

*Correspondence:

Georgios Charalambidis
gcharal@uoc.gr
Athanassios G. Coutsolelos
acoutsol@uoc.gr
Maylis Orio
maylis.orio@univ-amu.fr

Specialty section:

This article was submitted to
Catalysis and Photocatalysis,
a section of the journal
Frontiers in Chemistry

Received: 17 December 2018

Accepted: 20 May 2019

Published: 27 June 2019

Citation:

Panagiotakis S, Landrou G, Nikolaou V, Putri A, Hardré R, Massin J, Charalambidis G, Coutsolelos AG and Orio M (2019) Efficient Light-Driven Hydrogen Evolution Using a Thiosemicarbazone-Nickel (II) Complex. *Front. Chem.* 7:405. doi: 10.3389/fchem.2019.00405

In the following work, we carried out a systematic study investigating the behavior of a thiosemicarbazone-nickel (II) complex (**NiTSC-OMe**) as a molecular catalyst for photo-induced hydrogen production. A comprehensive comparison regarding the combination of three different chromophores with this catalyst has been performed, using $[\text{Ir}(\text{ppy})_2(\text{bpy})]\text{PF}_6$, $[\text{Ru}(\text{bpy})_3]\text{Cl}_2$ and $[\text{ZnTMePy}]\text{PCl}_4$ as photosensitizers. Thorough evaluation of the parameters affecting the hydrogen evolution experiments (i.e., concentration, pH, solvent nature, and ratio), has been performed in order to probe the most efficient photocatalytic system, which was comprised by **NiTSC-OMe** and $[\text{Ir}(\text{ppy})_2(\text{bpy})]\text{PF}_6$ as catalyst and chromophore, respectively. The electrochemical together with the photophysical investigation clarified the properties of this photocatalytic system and allowed us to propose a possible reaction mechanism for hydrogen production.

Keywords: light-driven hydrogen production, catalyst, nickel, molecular photosensitizer, photophysics

INTRODUCTION

One of the most important challenges of our society, that still lie ahead, is to discover renewable and abundant energy sources (Hosenuzzaman et al., 2015; Hosseini and Wahid, 2016). Solar energy is indeed an attractive and unlimited energy source which nonetheless requires the development of novel as well as efficient storage technologies (Styring, 2012; Tachibana et al., 2012; Faunce et al., 2013). Interestingly, hydrogen could unquestionably be applied for such a purpose: (i) it is the simplest and the most plentiful element on earth, (ii) the energy of the hydrogen-hydrogen bond is high, and (iii) it is considered as a non-polluting fuel (Peel, 2003). Hence, photocatalytic water splitting leading to hydrogen production is a method that without any doubt could be proved as an auspicious solution (Lewis and Nocera, 2006). Photocatalytic hydrogen production can be accomplished by systems containing a photosensitizer, a sacrificial electron donor and a catalyst (Ladomenou et al., 2015; Yuan et al., 2017). Nevertheless, there are plenty unsolved issues that still rest in the field of photocatalytic hydrogen production. Specifically, the development of systems utilizing earth-abundant materials with enhanced efficiency and durability (Wang and Sun, 2010; Du and Eisenberg, 2012). To that end, numerous hydrogen evolution catalysts along with a great number of different photosensitizers have been extensively examined over the last years (Tran et al., 2010, 2012; Du and Eisenberg, 2012; Wang et al., 2012; Sartorel et al., 2013).

Photocatalytic systems involving low-cost molecular catalysts and compounds prepared through easy synthetic approaches have been widely studied over the past decade (Artero et al., 2011; Eckenhoff et al., 2013; Ladomenou et al., 2015). Specifically, cobaloximes (Fihri et al., 2008; Lazarides et al., 2009, 2014; Du and Eisenberg, 2012; Landrou et al., 2016; Panagiotopoulos et al., 2016), and other polypyridine cobalt complexes have been applied as noble-metal-free catalysts (Eckenhoff et al., 2013; Yin et al., 2015; Zee et al., 2015). Although, several of these catalysts are efficient for photocatalytic hydrogen evolution reaction (HER), their stability was greatly limited upon visible light irradiation. Moreover, many researches draw inspiration from Nature trying to replicate the function of the hydrogenase enzymes (Lubitz et al., 2014; Brazzolotto et al., 2016), leading to the design of nickel complexes that were evaluated as molecular catalysts for HER. As a result, plenty nickel catalysts such as nickel bis(diphosphine) (DuBois and DuBois, 2009a,b; Helm et al., 2011; McLaughlin et al., 2011), and pyridinethiolate (Han et al., 2012, 2013; Rao et al., 2016) have been applied in such schemes, since they reproduce the structure of the active site of hydrogenase. Due to the effect of non-innocent ligands, (Han et al., 2012, 2013; Rao et al., 2015, 2016; Inoue et al., 2017) such nickel complexes have displayed excellent efficiency as catalyst reaching around 7,500 TON (Han et al., 2013; Rao et al., 2016). Thiosemicarbazone metal complexes are an emerging class of new HER electrocatalysts (Haddad et al., 2016, 2017; Straistari et al., 2017, 2018a,b) that have already been proved to be redox active (Blanchard et al., 2005; Haddad et al., 2017; Straistari et al., 2017) The presence of S-donors as well as N-atoms in thiosemicarbazone allows the protonation of the ligand and serve as proton relays (Campbell, 1975; DuBois, 2014; Coutard et al., 2016). One of the most essential aspect of light-driven proton reduction is the appropriate choice of the light-harvesting unit (i.e., photosensitizer, Ps). Despite the fact that $[\text{Ru}(\text{bpy})_3]\text{Cl}_2$ remains the most widely employed chromophore in such systems (Khnyzer et al., 2014; Lo et al., 2016), iridium complexes are still the most efficient entities found in several photocatalytic systems (Goldsmith et al., 2005; Andreiadis et al., 2011). Additionally, porphyrins and other tetrapyrrolic derivatives can be effective candidates for HER due to their unique stability, electrochemical properties, and appropriate energy levels (Ladomenou et al., 2015). For this reason, various metalloporphyrins such as Zn(II) or Sn(IV), have been utilized as photosensitizers for photocatalytic HER over the years (Lazarides et al., 2014; Kuposova et al., 2016; Landrou et al., 2016; Queyriaux et al., 2018).

Here we will discuss the implications of our findings regarding a novel photoinduced HER scheme using a noble-metal-free bis-thiosemicarbazone nickel (II) complex (Straistari et al., 2017), namely NiTSC-OMe. In this study, three different light harvesting complexes, $[\text{Ir}(\text{ppy})_2(\text{bpy})]\text{PF}_6$ (Ps1), $[\text{Ru}(\text{bpy})_3]\text{Cl}_2$ (Ps2), and $[\text{ZnTMePy}]\text{PCL}_4$ (Ps3) (Andriadis et al., 2011; Lazarides et al., 2014; Natali et al., 2014) were used as photosensitizers and trimethylamine (TEA) as the sacrificial electron donor (Figure 1). The efficiency of the resulting photocatalytic system was optimized by studying different concentrations of the catalyst, the effect of solvent mixture, the

solvent ratio, and the influence of pH in the buffer solution. The electron transfer processes that occur were examined through fluorescence spectroscopic techniques. To solidify the photochemical stability of our system, regeneration experiments were conducted and the homogeneous nature of our catalytic system was proved using poisoning experiments. Based on the results gathered from these studies we were finally able to propose a possible reaction mechanism for light-driven hydrogen production with our photocatalytic system.

EXPERIMENTAL SECTION

Materials and Methods

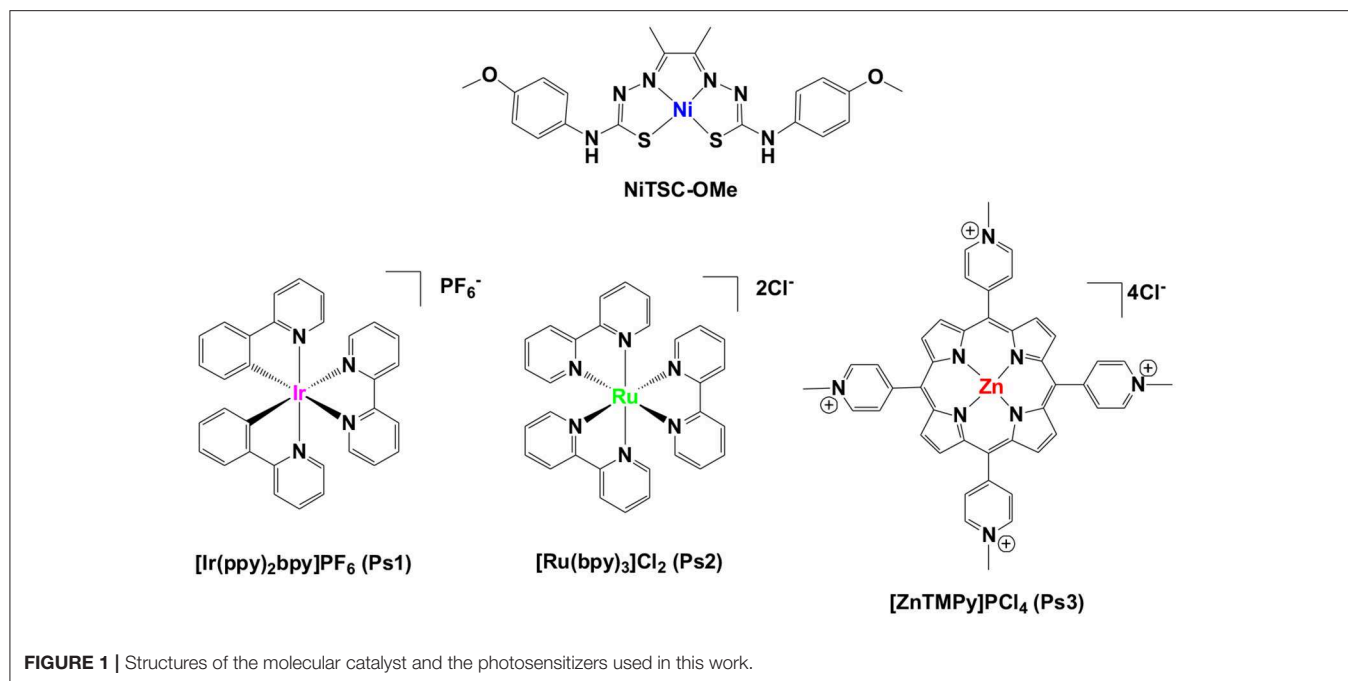
Reagents and solvents were purchased as reagent grade from usual commercial sources and were used without further purification, unless otherwise stated. $[\text{Ir}(\text{ppy})_2(\text{bpy})]\text{PF}_6$ and $[\text{Ru}(\text{bpy})_3]\text{Cl}_2$ were purchased from commercial sources and used without further purification. The nickel thiosemicarbazone complex (NiTSC-OMe) (Straistari et al., 2017) and the Zinc (II) *meso*-tetrakis (1-methylpyridinium-4-yl) porphyrin tetrachloride ($[\text{ZnTMePy}]\text{PCL}_4$) (Lazarides et al., 2014) were prepared as previously reported.

Photophysical Measurements

UV-Vis absorption spectra were measured on a Shimadzu UV-1700 spectrophotometer using 10 mm path-length cuvettes (Figure S1). The emission spectra were measured by exciting the samples at 337 nm using a JASCO FP-6500 fluorescence spectrophotometer equipped with a red sensitive WRE-343 photomultiplier tube (wavelength range 200–850 nm).

Photocatalytic HER Experiments

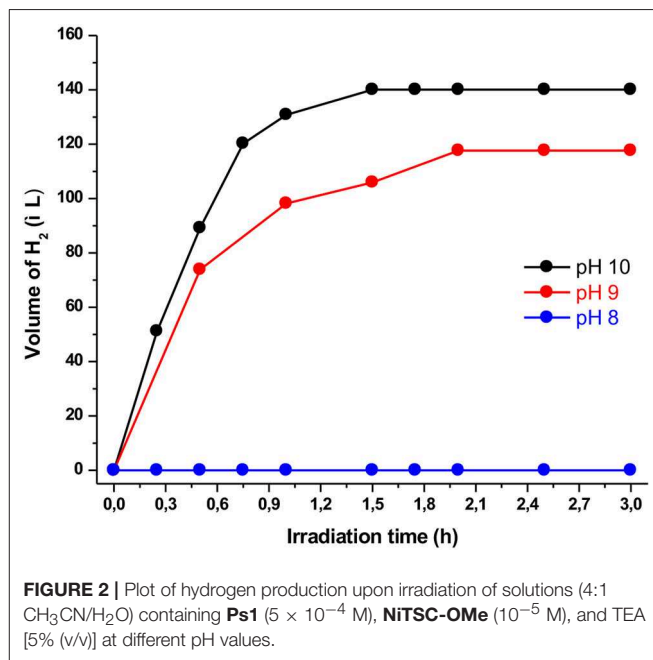
For the photoinduced HER studies, each sample was prepared in a 42 mL glass vial with silicone septum. The buffer solutions were prepared by dissolving the sacrificial electron donor [triethylamine (TEA) or ascorbic acid (AA)] in water. It was necessary to add a small amount of acetonitrile in order to obtain a homogeneous solution. The pH was adjusted to the required value using concentrated HCl or NaOH solutions. Then the organic solvent (CH_3CN or EtOH) was added in order to obtain the desired ratio. For the sample preparation, the chromophore was dissolved in the buffer solution and consequently a solution of the catalyst in CH_3CN or EtOH was added. The final volume of the sample was 5 mL and the mixture was degassed for 10 min using nitrogen. The vials were sealed and the samples irradiated with a white LED lamp (power of 40 W, color temperature of 6,400 K and lumen of 3,800 LM, Figure S2). The amounts of produced hydrogen were determined by gas chromatography (external standard technique) using a Shimadzu GC-2010 plus chromatograph with a TCD detector and a molecular sieve 5 Å column (30–0.53 mm). Gas samples of 100 μL were taken from the headspace and injected immediately into the GC. In all cases, the reported results are the average of three independent experiments. The TONs were calculated using the produced moles of hydrogen vs. the moles of the catalyst. Control experiments were performed under the same conditions after the removal of the catalyst from the hydrogen generating system.



Mercury poisoning experiments were performed, in order to examine the possible formation of metallic nanoparticles or colloids during the hydrogen evolution process. In these studies, an excess of mercury (ca. 40 equiv.) was added to the hydrogen evolution solutions (prepared with the above mentioned procedure).

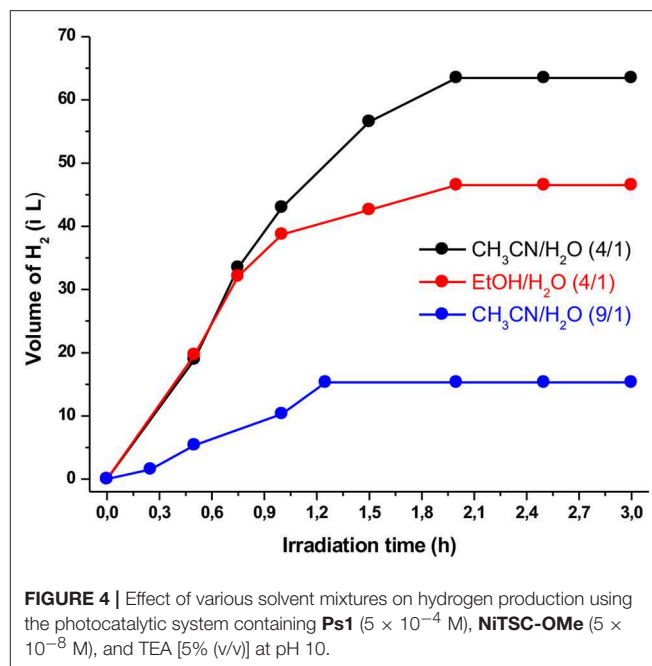
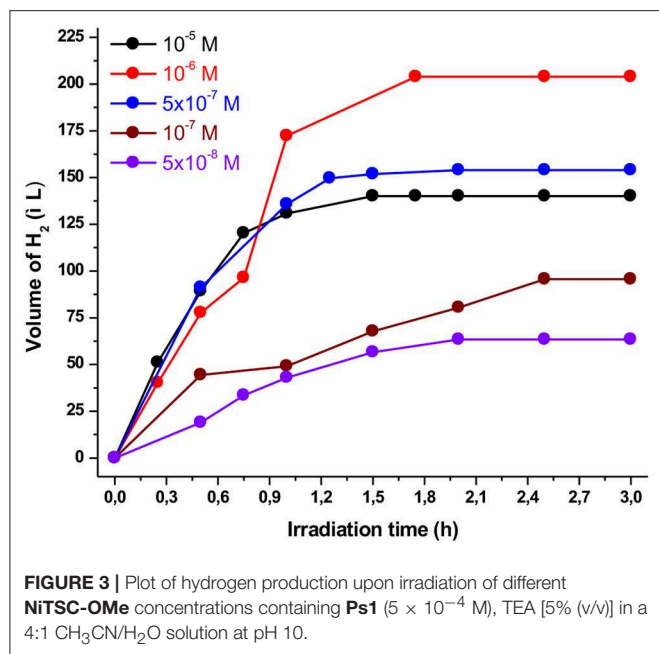
RESULTS AND DISCUSSION

In our recent work, we reported the synthesis of a novel nickel catalyst (NiTSC-OMe, **Figure 1**) that exhibits high electrocatalytic activity for proton reduction to dihydrogen (Straistari et al., 2017). Based on these encouraging results we wanted to examine the capability of this catalyst toward photochemical hydrogen production. Thus, in the present study three different chromophores (**Figure 2**) were tested as photosensitizers and combined with the NiTSC-OMe catalyst to determine its ability as an effective photocatalytic system to reduce protons into hydrogen. We have analyzed various parameters, such as the concentration of the catalyst (10^{-5} – 5×10^{-8} M), the pH of the buffer solution, the effect of the solvent ratio in the photocatalytic mixture and the stability of our system. We carried out several experiments using TEA [5% (v/v)] or AA (0.2 M) as the sacrificial electron donors in various pH buffers (from pH = 2.5 to pH = 10). In addition, different concentrations of the catalyst and the chromophore were tested using varied solvent mixtures. Notably, in all cases no hydrogen production was observed using $[\text{Ru}(\text{bpy})_3]^{2+}$ (**Ps2**) or $[\text{ZnTMePy}]^+$ (**Ps3**) as photosensitizers. However, when $[\text{Ir}(\text{ppy})_2(\text{bpy})]^+$ (**Ps1**) was used as photosensitizer and TEA [5% (v/v)] as sacrificial electron donor, a photocatalytic hydrogen evolution of 140 μL from 1 ml of H_2O was recorded, highlighting once more that the



photosensitizer is an essential component in such photocatalytic HER systems.

In the above mentioned system, the first parameter that we examined was the effect of the protons concentration (pH). In detail, we used three different buffer solutions with pH values of 8, 9, and 10, concluding that the optimum one was at pH = 10. As presented in **Figure 2** using the solution with pH = 8, no hydrogen production was observed after 3 h of irradiation. On the contrary, using buffer solutions of pH = 9



and pH = 10 we detected hydrogen production of 105 and 125 TONs, respectively. These findings are consistent with results derived from similar systems in which the optimum pH value is close to the pKa value of the sacrificial electron donor. Namely, in our case since the pKa of TEA is 10.7, the optimum pH of the buffer solution was expected at pH = 10 (Pellegrin and Odobel, 2017). Moreover, at pH values lower than its pKa value TEA is protonated and loses its electron donating ability (Rao et al., 2016).

Furthermore, the performances of the photocatalytic HER systems strongly depend on the catalyst concentration as well as the relative ratio between the photosensitizer and the catalyst. Accordingly, we kept the concentration of the Ps1 photosensitizer constant (5×10^{-4} M), while the concentration of the catalyst varied from 10^{-5} to 5×10^{-8} M. As illustrated in **Figure 3**, the volume of the produced H₂ was increased when the concentration of the catalyst decreased from 10^{-5} to 10^{-6} M, reaching a maximum of 204 μ L. In addition, further decrease in the concentration of the catalyst (5×10^{-7} – 5×10^{-8}) resulted in lower catalytic efficiency. On the other hand, the catalytic activity of the system (TON) was increased when the concentration of the catalyst decreased from 10^{-5} to 5×10^{-8} M (**Figure S4**). Notably, when the concentration of the NiTSC-OMe was 5×10^{-8} M the system displayed the maximum TON and TOF values, namely 11,333 and 7,971, respectively (see **Table S1**). These results are in contrast with our previous work (Lazarides et al., 2014; Panagiotopoulos et al., 2016), where the maximum photocatalytic activity was observed when the concentration of the catalyst was in excess compared to that of the photosensitizer. This behavior can be attributed to two possible reasons: (i) the quenching of the excited state of the Ps1 by the NiTSC-OMe complex and (ii) the great difference in the molecular absorptivity (ϵ) of complexes. Concerning the first hypothesis,

since the reductive quenching process of photosensitizer by the catalyst is in competition with the expected reaction with TEA, decreasing the catalyst concentration will possibly favor the suggested reductive pathway. Moreover, regarding the second probable assumption, in our previous work the photosensitizer [ZnTMePy]⁺ exhibited an absorption coefficient of $\epsilon = 1,80,000 \text{ M}^{-1} \cdot \text{cm}^{-1}$. In the present study though, the Ps1 exhibits an absorption coefficient of $\epsilon = 6000 \text{ M}^{-1} \cdot \text{cm}^{-1}$ (Andreiadis et al., 2011), and the catalyst (NiTSC-OMe) displays an absorption band at 470 nm with an epsilon value of $\epsilon = 17,000 \text{ M}^{-1} \cdot \text{cm}^{-1}$ (Straistari et al., 2017). Consequently, the absorption properties of the catalyst can reduce the available photons for the photosensitizer, thus the catalyst concentration should be lower than that of the photosensitizer in order for the system to be more efficient.

The nature as well as the ratio of the solvents definitely plays a significant role in the HER. As a result, we examined two different solvent mixtures, i.e., CH₃CN/H₂O and Ethanol/H₂O, using also different ratio (from 4:1 to 9:1). As shown in **Figure 4**, the best solvent mixture was found to be CH₃CN/H₂O in a 4:1 ratio producing a maximum volume of hydrogen of 63 μ L after almost 2 h of irradiation. We concluded that the solvent ratio induced critical changes on the hydrogen production, most likely because affecting the solubility properties. These solubility properties can be altered via the dielectric constant and the diffusion coefficient of each solvent (Rao et al., 2015; Pellegrin and Odobel, 2017). When CH₃CN/H₂O in a 9:1 ratio was utilized as the solvent mixture, the photocatalytic performance dramatically decreased. The smaller water concentration probably leads to lower solubility with direct impact on the photocatalytic activity of the system.

In all presented photocatalytic experiments, H₂ production stops after almost 2 h of irradiation. Therefore, regeneration

and photolysis experiments have been performed in order to examine the stability of our system (**Figure 5** and **Figure S3**). As illustrated in **Figure 5** (right part), we performed UV-Vis absorption photolysis experiment in a solution containing **Ps1** and **NiTSC-OMe**. The characteristic absorption bands of our system (416 for **Ps1** and 460 nm for **NiTSC-OMe**) were significantly decreased after 15 min of irradiation, suggesting bleaching of the photolysis solutions. After the addition of either the catalyst or the photosensitizer we didn't observe any hydrogen evolution. However, when both components were added to the reaction mixture, the catalytic system was effectively regenerated, leading to 3,067 TON (**Figure 5**, left), suggesting that both these components undergo concomitant decomposition after almost 2 h of irradiation.

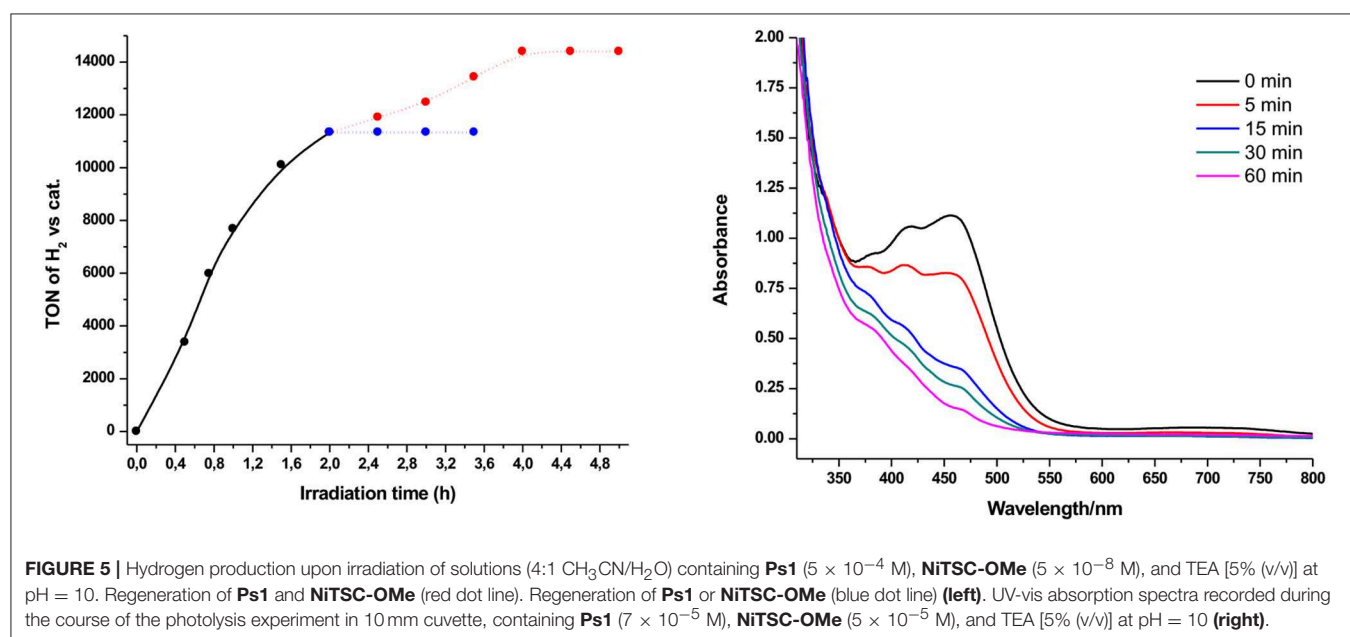
The degraded compounds can form metallic nanoparticles, which can act as the catalytic species during HER (Lazarides et al., 2014). In order to exclude this possibility we performed mercury poisoning experiments. Photocatalytic experiments in the presence of mercury showed no significant change in the amount of the produced H_2 (11,787 TONs), thus confirming the homogeneous nature of our photocatalytic system.

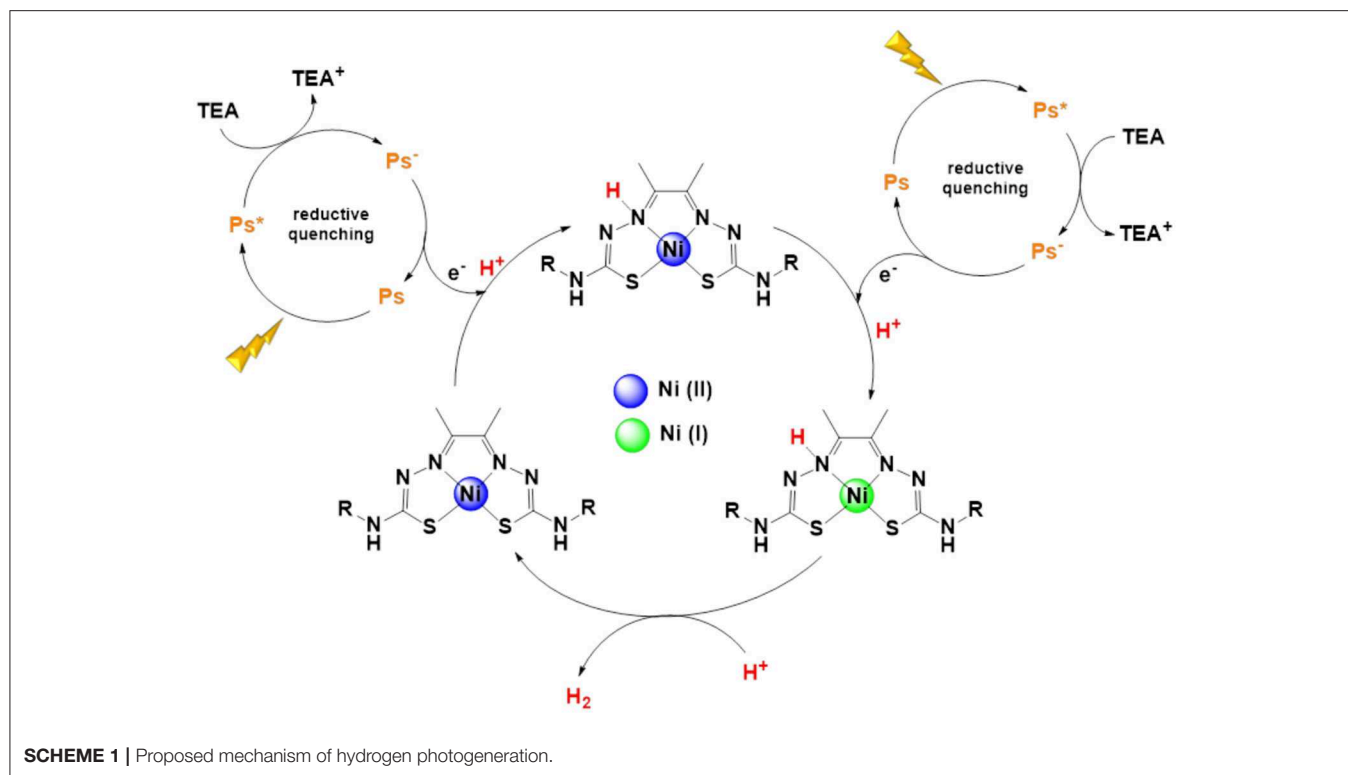
To shed light into the mechanism of photocatalytic system, fluorescence spectroscopy was used. Specifically, emission spectroscopy experiments were carried out using **Ps1** (4×10^{-5} M) as photosensitizer upon its excitation at 337 nm in CH_3CN solution. While the photocatalytic measurements were performed in a CH_3CN/H_2O mixture, the photophysical studies were carried out using CH_3CN as a solvent. This is due to the fact that TEA was not soluble enough in the high concentrations needed for the Stern Volmer plots in the CH_3CN/H_2O mixture. Firstly, we examined the quenching process on **Ps1** by increasing the concentration of either TEA ($0 \rightarrow 0.36$ M)] (**Figure S5**,

left) or **NiTSC-OMe** ($0 \rightarrow 4.1 \times 10^{-5}$ M) (**Figure S6**, left). In addition, we have calculated the Stern-Volmer constant (K_{SV}) based on Stern-Volmer plot (**Figures S4, S5**, right), using the equation $I_0/I = 1 + K_{SV}[Q]$, where I_0 and I are the fluorescence intensities observed in the absence and in the presence of each quencher, respectively, and $[Q]$ is defined as the quencher concentration (Keizer, 1983). In perfect agreement with previous publications, the K_{SV} constant was higher in the case of the catalyst ($K_{SV} = 13,419.5 \text{ M}^{-1}$) compared to the TEA ($K_{SV} = 11.7 \text{ M}^{-1}$). Moreover, we calculated the quenching constant for

TABLE 1 | Redox potentials (V vs. NHE) of the different compounds employed in this study (Ps^* represents the excited state of Ps : Ps^+ and Ps^- , its oxidized and reduced forms, respectively) together with the thermodynamic driving forces for the different electron transfer processes ($\Delta G^1(Ps/Cat)$, $\Delta G^2(Ps/Cat)$, and $\Delta G(SED/PS)$, eV).

Photosensitizers	$E(Ps^+/Ps^*)$	$E(Ps/Ps^-)$	$E(Ps^+/Ps)$	$E(Ps^*/Ps^-)$
Ps1	-0.60	-1.17	+1.50	+0.93
$\Delta G^1(Ps/Cat)$	+0.44	-0.13		
$\Delta G^2(Ps/Cat)$	+1.07	+0.50		
$\Delta G(SED/PS)$			-0.57	0
Ps2	-0.86	-1.28	+1.26	+0.84
$\Delta G^1(Ps/Cat)$	+0.18	-0.24		
$\Delta G^2(Ps/Cat)$	+0.81	+0.39		
$\Delta G(SED/PS)$			-0.33	+0.09
Ps3	-0.45	-0.85	+1.18	+0.78
$\Delta G^1(Ps/Cat)$	+0.26	+0.20		
$\Delta G^2(Ps/Cat)$	+1.22	+0.82		
$\Delta G(SED/PS)$			-0.25	+0.15
Catalyst	$E(Ni^{II}/Ni^I)$	$E(Ni^I/L^-)$	SED	E_{Ox}
NiTSC-OMe	-1.04	-1.67	TEA	0.93





NiTSC-OMe ($K_Q = 4.99 \times 10^{10} \text{ M}^{-1}\text{s}^{-1}$) and for TEA ($K_Q = 4.35 \times 10^7 \text{ M}^{-1}\text{s}^{-1}$) as well, which are derived from the equation: $K_{SV} = K_Q \tau$, where τ stands for the excited state lifetime in the absence of the quencher (Han et al., 2013; Yuan et al., 2016). However, under similar conditions to the H_2 production experiments in the emission spectra of **Ps1**, we observe that the characteristic fluorescence peak of the photosensitizer (at 590 nm) decreases only when the sacrificial electron donor (TEA) is added (Figure S7). What is more, there is a great difference in the quenching process, namely 50% in case of TEA and 1% in case of the catalyst. Therefore, even though, the rate constant by the **NiTSC-OMe** is greater than the rate constant by TEA, the major electron transfer pathway occurs from the excited photosensitizer to TEA, since the concentration of electron donor is bigger than that of the catalyst in the system (Han et al., 2013). In summary, hydrogen production in our system is initiated via reductive quenching of the photosensitizer.

The redox potentials of the reported compounds used in this study are listed in Table 1. Based on these values the thermodynamic driving forces for the different electron transfer processes, $\Delta G^1(\text{PS}/\text{Cat})$, were calculated [(Queyriaux et al., 2017) and references herein, Goldsmith et al., 2005]. The resulting $\Delta G^1(\text{PS}/\text{Cat})$ values turn out to be in agreement with the fluorescence quenching measurements which seems to indicate that the initial step is the reductive quenching of the photosensitizer. Indeed, the calculated $\Delta G^1(\text{PS}/\text{Cat})$ values are positive for a reduction from Ps^+/Ps^* for **Ps1** and **Ps2** (+0.44 and +0.18, respectively) whereas they are negative for a reduction from Ps/Ps^- (-0.13 and -0.24, respectively). It is also possible

to find that whatever the mechanism is, the **Ps3** potentials are not negative enough to reduce the nickel catalyst, which would explain the observed lack of photocatalytic activity. The double reduction of the catalyst is also unlikely since the values of $\Delta G^2(\text{PS}/\text{Cat})$ are largely positive ($> +0.40 \text{ eV}$) which would not be in favor an EECC mechanism (E corresponds to an electron transfer step and C to a chemical reaction, here protonation). Finally, the difference in activity between **Ps1** and **Ps2** does not seem to be rationalized by the little difference in driving force of injection (respectively, -0.13 and -0.24 eV), but rather by the difference of driving regeneration force $\Delta G(\text{SED}/\text{PS})$ which is larger in the case of **Ps2** than for **Ps1** (respectively, +0.09 and 0 eV).

Taking into consideration all studies reported in this work, we propose a possible H_2 production mechanism as illustrated in Scheme 1. First, $[\text{Ir}(\text{ppy})_2(\text{bpy})]^+$ (**Ps**) is excited by visible light irradiation to form the excited state of the photosensitizer (Ps^*). Subsequently, the sacrificial electron donor (TEA) transfers an electron to the excited photosensitizer via reductive quenching process forming its oxidized state (TEA^+) and the reduced state of the photosensitizer (Ps^-) (Scheme 1).

Then, a protonation of coordinated N-atom of the ligand on nickel complex takes place (Straistari et al., 2017) followed by an electron transfer process from the photosensitizer (Ps^-) to the nickel catalyst, creating the nickel (I) complex and forming an hydride intermediate as presented in the scheme below. Finally, H_2 production from the system through the nickel catalyst occurs together with its regeneration.

CONCLUSIONS

In summary, a systematic photocatalytic study toward light-driven hydrogen production is presented herein, using three different chromophores and one bis-thiosemicarbazone nickel complex. When NiTSC-OMe was combined with either Ps2 or Ps3, no hydrogen production was observed under various experimental conditions. However, when Ps1 was utilized as a chromophore, H₂ production was detected. In order to estimate the optimal conditions we examined the influence of various parameters: the concentration of the catalyst, the pH value of the buffer solution and the ratio as well as the nature of the solvent mixture. Overall, the highest amount of H₂ (204 μL), was attained using a 4:1 CH₃CN/H₂O solution containing NiTSC-OMe (10⁻⁶ M), Ps1 (5 × 10⁻⁴ M), TEA [5% (v/v)] at pH 10. The maximum catalytic activity of the system though, with the highest TON and TOF values (11,333 and 7,971) were observed using NiTSC-OMe (5 × 10⁻⁸ M), Ps1 (5 × 10⁻⁴ M), TEA [5% (v/v)] at pH 10 in 4:1 CH₃CN/H₂O solution. All the promising results displayed in this study offer new aspects regarding the combination of chromophores with nickel catalysts for hydrogen production. In addition, such efforts could in general provide new perspectives improving the efficiency and the function of catalytic systems developed for photoinduced hydrogen evolution using water.

REFERENCES

- Andreiadis, E. S., Chavarot-Kerlidou, M., Fontecave, M., and Artero, V. (2011). Artificial photosynthesis: from molecular catalysts for light-driven water splitting to photoelectrochemical cells. *Photochem. Photobiol.* 87, 946–964. doi: 10.1111/j.1751-1097.2011.00966.x
- Artero, V., Chavarot-Kerlidou, M., and Fontecave, M. (2011). Splitting water with cobalt. *Angewandte Chemie* 50, 7238–7266. doi: 10.1002/anie.2011007987
- Blanchard, S., Neese, F., Bothe, E., Bill, E., Weyhermüller, T., and Wieghardt, K. (2005). Square planar vs tetrahedral coordination in diamagnetic complexes of nickel(II) containing two bidentate pi-radical monoanions. *Inorg. Chem.* 44, 3636–3656. doi: 10.1021/ic040117e
- Brazzolotto, D., Gennari, M., Queyriaux, N., Simmons, T. R., Pecauc, J., Demeshko, S., et al. (2016). Nickel-centred proton reduction catalysis in a model of [NiFe] hydrogenase. *Nat. Chem.* 8, 1054–1060. doi: 10.1038/nchem.2575
- Campbell, M. J. M. (1975). Transition-metal complexes of thiosemicarbazide and thiosemicarbazones. *Coord. Chem. Rev.* 15, 279–319. doi: 10.1016/S0010-8545(00)80276-3
- Coutard, N., Kaeffer, N., and Artero, V. (2016). Molecular engineered nanomaterials for catalytic hydrogen evolution and oxidation. *Chem. Commun.* 52, 13728–13748. doi: 10.1039/C6CC06311J
- Du, P. W., and Eisenberg, R. (2012). Catalysts made of earth-abundant elements (Co, Ni, Fe) for water splitting: Recent progress and future challenges. *Energy Environ. Sci.* 5, 6012–6021. doi: 10.1039/c2ee03250c
- DuBois, D. L. (2014). Development of molecular electrocatalysts for energy storage. *Inorg. Chem.* 53, 3935–3960. doi: 10.1021/ic4026969
- DuBois, M. R., and DuBois, D. L. (2009a). Development of molecular electrocatalysts for CO₂ reduction and H₂ production/oxidation. *Acc. Chem. Res.* 42, 1974–1982. doi: 10.1021/ar900110c
- DuBois, M. R., and DuBois, D. L. (2009b). The roles of the first and second coordination spheres in the design of molecular catalysts for H₂ production and oxidation. *Chem. Soc. Rev.* 38, 62–72. doi: 10.1039/B801197B
- Eckenhoff, W. T., Mcnamara, W. R., Du, P. W., and Eisenberg, R. (2013). Cobalt complexes as artificial hydrogenases for the reductive side of water splitting. *Biochim. Biophys. Acta* 1827, 958–973. doi: 10.1016/j.bbabi.2013.05.003

AUTHOR CONTRIBUTIONS

MO and AC designed and directed the study. AP synthesized the catalyst. SP, GL, and VN performed the experiments. RH, JM, GC, AC, and MO analyzed the data. GC, AC, and MO wrote the paper with input from all authors. All authors contributed to the design and implementation of the research, to the analysis of the results and to the writing of the manuscript.

ACKNOWLEDGMENTS

General Secretariat for Research and Technology (GSRT) and Hellenic Foundation for Research and Innovation (HFRI) (project code: 508) are gratefully acknowledged for the financial support of this research. Also, the European Commission's Seventh Framework Program (FP7/2007-2013) under grant agreement no. 229927 (FP7-REGPOT-2008-1, Project BIO-SOLENUTI), and the Special Research Account of the University of Crete.

SUPPLEMENTARY MATERIAL

The Supplementary Material for this article can be found online at: <https://www.frontiersin.org/articles/10.3389/fchem.2019.00405/full#supplementary-material>

- Faunce, T. A., Lubitz, W., Rutherford, A. W., Macfarlane, D. R., Moore, G. F., Yang, P. D., et al. (2013). Energy and environment policy case for a global project on artificial photosynthesis. *Energy Environ. Sci.* 6, 695–698. doi: 10.1039/c3ee00063j
- Fihri, A., Artero, V., Razavet, M., Baffert, C., Leibl, W., and Fontecave, M. (2008). Cobaloxime-based photocatalytic devices for hydrogen production. *Angewandte Chemie* 47, 564–567. doi: 10.1002/anie.200702953
- Goldsmith, J. I., Hudson, W. R., Lowry, M. S., Anderson, T. H., and Bernhard, S. (2005). Discovery and high-throughput screening of heteroleptic iridium complexes for photoinduced hydrogen production. *J. Am. Chem. Soc.* 127, 7502–7510. doi: 10.1021/ja0427101
- Haddad, A. Z., Cronin, S. P., Mashuta, M. S., Buchanan, R. M., and Grapperhaus, C. A. (2017). Metal-assisted ligand-centered electrocatalytic hydrogen evolution upon reduction of a Bis(thiosemicarbazonato)Cu(II) complex. *Inorg. Chem.* 56, 11254–11265. doi: 10.1021/acs.inorgchem.7b01608
- Haddad, A. Z., Garabato, B. D., Kozłowski, P. M., Buchanan, R. M., and Grapperhaus, C. A. (2016). Beyond metal-hydrides: non-transition-metal and metal-free ligand-centered electrocatalytic hydrogen evolution and hydrogen oxidation. *J. Am. Chem. Soc.* 138, 7844–7847. doi: 10.1021/jacs.6b04441
- Han, Z., Mcnamara, W. R., Eum, M. S., Holland, P. L., and Eisenberg, R. (2012). A nickel thiolate catalyst for the long-lived photocatalytic production of hydrogen in a noble-metal-free system. *Angewandte Chemie* 51, 1667–1670. doi: 10.1002/anie.201107329
- Han, Z., Shen, L., Brennessel, W. W., Holland, P. L., and Eisenberg, R. (2013). Nickel pyridinethiolate complexes as catalysts for the light-driven production of hydrogen from aqueous solutions in noble-metal-free systems. *J. Am. Chem. Soc.* 135, 14659–14669. doi: 10.1021/ja405257s
- Helm, M. L., Stewart, M. P., Bullock, R. M., DuBois, M. R., and DuBois, D. L. (2011). A synthetic nickel electrocatalyst with a turnover frequency above 100,000 s⁻¹ for H₂ production. *Science* 333, 863–866. doi: 10.1126/science.1205864
- Hosenuzzaman, M., Rahim, N. A., Selvaraj, J., Hasanuzzaman, M., Malek, A. B. M. A., and Nahar, A. (2015). Global prospects, progress, policies, and environmental impact of solar photovoltaic power generation. *Renew. Sust. Energy Rev.* 41, 284–297. doi: 10.1016/j.rser.2014.08.046

- Hosseini, S. E., and Wahid, M. A. (2016). Hydrogen production from renewable and sustainable energy resources: Promising green energy carrier for clean development. *Renew. Sust. Energy Rev.* 57, 850–866. doi: 10.1016/j.rser.2015.12.112
- Inoue, S., Mitsuhashi, M., Ono, T., Yan, Y. N., Kataoka, Y., Handa, M., et al. (2017). Photo- and electrocatalytic hydrogen production using valence isomers of N2S2-type nickel complexes. *Inorg. Chem.* 56, 12129–12138. doi: 10.1021/acs.inorgchem.7b01244
- Keizer, J. (1983). Non-linear fluorescence quenching and the origin of positive curvature in Stern-Volmer plots. *J. Am. Chem. Soc.* 105, 1494–1498. doi: 10.1021/ja00344a013
- Khayzer, R. S., Thoi, V. S., Nippe, M., King, A. E., Jurss, J. W., El Roz, K. A., et al. (2014). Towards a comprehensive understanding of visible-light photogeneration of hydrogen from water using cobalt(II) polypyridyl catalysts. *Energy Environ. Sci.* 7, 1477–1488. doi: 10.1039/C3EE43982H
- Koposova, E., Liu, X., Pendin, A., Thiele, B., Shumilova, G., Ermolenko, Y., et al. (2016). Influence of meso-substitution of the porphyrin ring on enhanced hydrogen evolution in a photochemical system. *J. Phys. Chem. C* 120, 13873–13890. doi: 10.1021/acs.jpcc.6b01467
- Ladomenou, K., Natali, M., Iengo, E., Charalampidis, G., Scandola, F., and Coutsolelos, A. G. (2015). Photochemical hydrogen generation with porphyrin-based systems. *Coord. Chem. Rev.* 304, 38–54. doi: 10.1016/j.ccr.2014.10.001
- Landrou, G., Panagiotopoulos, A. A., Ladomenou, K., and Coutsolelos, A. G. (2016). Photochemical hydrogen evolution using Sn-porphyrin as photosensitizer and a series of Cobaloximes as catalysts. *J. Porphyr. Phthalocyanines* 20, 534–541. doi: 10.1142/S1088424616500243
- Lazarides, T., Delor, M., Sazanovich, I. V., McCormick, T. M., Georgakaki, I., Charalambidis, G., et al. (2014). Photocatalytic hydrogen production from a noble metal free system based on a water soluble porphyrin derivative and a cobaloxime catalyst. *Chem. Commun.* 50, 521–523. doi: 10.1039/C3CC45025B
- Lazarides, T., McCormick, T., Du, P., Luo, G., Lindley, B., and Eisenberg, R. (2009). Making hydrogen from water using a homogeneous system without noble metals. *J. Am. Chem. Soc.* 131, 9192–9194. doi: 10.1021/ja903044n
- Lewis, N. S., and Nocera, D. G. (2006). Powering the planet: Chemical challenges in solar energy utilization. *Proc. Natl. Acad. Sci. U. S. A.* 103, 15729–15735. doi: 10.1073/pnas.0603395103
- Lo, W. K. C., Castillo, C. E., Gueret, R., Fortage, J., Rebarz, M., Sliwa, M., et al. (2016). Synthesis, characterization, and photocatalytic H₂-evolving activity of a family of [Co(N4Py)(X)](n+) complexes in aqueous solution. *Inorg. Chem.* 55, 4564–4581. doi: 10.1021/acs.inorgchem.6b00391
- Lubitz, W., Ogata, H., Rudiger, O., and Reijerse, E. (2014). Hydrogenases. *Chem. Rev.* 114, 4081–4148. doi: 10.1021/cr4005814
- McLaughlin, M. P., McCormick, T. M., Eisenberg, R., and Holland, P. L. (2011). A stable molecular nickel catalyst for the homogeneous photogeneration of hydrogen in aqueous solution. *Chem. Commun.* 47, 7989–7991. doi: 10.1039/c1cc12347e
- Natali, M., Luisa, A., Lengo, E., and Scandola, F. (2014). Efficient photocatalytic hydrogen generation from water by a cationic cobalt(II) porphyrin. *Chem. Commun.* 50, 1842–1844. doi: 10.1039/c3cc48882a
- Panagiotopoulos, A., Ladomenou, K., Sun, D., Artero, V., and Coutsolelos, A. G. (2016). Photochemical hydrogen production and cobaloximes: the influence of the cobalt axial N-ligand on the system stability. *Dalton Transact.* 45, 6732–6738. doi: 10.1039/C5DT04502A
- Peel, M. (2003). *The Hydrogen Economy: The Creation of the Worldwide Energy Web and the Redistribution of Power on Earth*. Tls-the Times Literary Supplement, 5227 29–29.
- Pellegrin, Y., and Odobel, F. (2017). Sacrificial electron donor reagents for solar fuel production. *Comptes Rendus Chimie* 20, 283–295. doi: 10.1016/j.crci.2015.11.026
- Queyriaux, N., Giannoudis, E., Windle, C. D., Roy, S., Pecauc, J., Coutsolelos, A. G., et al. (2018). A noble metal-free photocatalytic system based on a novel cobalt tetrapyridyl catalyst for hydrogen production in fully aqueous medium. *Sustain. Energy Fuels* 2, 553–557. doi: 10.1039/C7SE00428A
- Queyriaux, N., Wahyuno, R. A., Fize, J., Gablin, C., Wächtler, M., Martinez, E., et al. (2017). Aqueous photocurrent measurements correlated to ultrafast electron transfer dynamics at ruthenium tris diimine sensitized NiO photocathodes. *J. Phys. Chem. C* 121, 5891–5904. doi: 10.1021/acs.jpcc.6b12536
- Rao, H., Wang, Z. Y., Zheng, H. Q., Wang, X. B., Pan, C. M., Fan, Y. T., et al. (2015). Photocatalytic hydrogen evolution from a cobalt/nickel complex with dithiolenic ligands under irradiation with visible light. *Catal. Sci. Technol.* 5, 2332–2339. doi: 10.1039/C4CY01574F
- Rao, H., Yu, W. Q., Zheng, H. Q., Bonin, J., Fan, Y. T., and Hou, H. W. (2016). Highly efficient photocatalytic hydrogen evolution from nickel quinolinethiolate complexes under visible light irradiation. *J. Power Sourc.* 324, 253–260. doi: 10.1016/j.jpowsour.2016.05.095
- Sartorel, A., Bonchio, M., Campagna, S., and Scandola, F. (2013). Tetrametallic molecular catalysts for photochemical water oxidation. *Chem. Soc. Rev.* 42, 2262–2280. doi: 10.1039/C2CS35287G
- Straistari, T., Fize, J., Shova, S., Reglier, M., Artero, V., and Orio, M. (2017). A Thiosemicarbazone-nickel(II) complex as efficient electrocatalyst for hydrogen evolution. *Chemcatchem* 9, 2262–2268. doi: 10.1002/cctc.201600967
- Straistari, T., Hardré, R., Fize, J., Shova, S., Giorgi, M., Réglie, M., et al. (2018a). Hydrogen evolution reactions catalyzed by a bis(thiosemicarbazone) cobalt complex: an experimental and theoretical study. *Chem. Euro. J.* 24, 8779–8786. doi: 10.1002/chem.201801155
- Straistari, T., Hardre, R., Massin, J., Attolini, M., Faure, B., Giorgi, M., et al. (2018b). Influence of the metal ion on the electrocatalytic hydrogen production by a thiosemicarbazone palladium complex. *Euro. J. Inorg. Chem.* 2259–2266. doi: 10.1002/ejic.201800120
- Styring, S. (2012). Artificial photosynthesis for solar fuels. *Faraday Discuss.* 155, 357–376. doi: 10.1039/C1FD00113B
- Tachibana, Y., Vayssieres, L., and Durrant, J. R. (2012). Artificial photosynthesis for solar water-splitting. *Nat. Photonics* 6, 511–518. doi: 10.1038/nphoton.2012.175
- Tran, P. D., Artero, V., and Fontecave, M. (2010). Water electrolysis and photoelectrolysis on electrodes engineered using biological and bio-inspired molecular systems. *Energy Environ. Sci.* 3, 727–747. doi: 10.1039/b926749b
- Tran, P. D., Wong, L. H., Barber, J., and Loo, J. S. C. (2012). Recent advances in hybrid photocatalysts for solar fuel production. *Energy Environ. Sci.* 5, 5902–5918. doi: 10.1039/c2ee02849b
- Wang, M., Chen, L., and Sun, L. C. (2012). Recent progress in electrochemical hydrogen production with earth-abundant metal complexes as catalysts. *Energy Environ. Sci.* 5, 6763–6778. doi: 10.1039/c2ee03309g
- Wang, M., and Sun, L. C. (2010). Hydrogen production by noble-metal-free molecular catalysts and related nanomaterials. *ChemSuschem* 3, 551–554. doi: 10.1002/cssc.201000062
- Yin, M. C., Ma, S., Wu, C. J., and Fan, Y. T. (2015). A noble-metal-free photocatalytic hydrogen production system based on cobalt(III) complex and eosin Y-sensitized TiO₂. *Rsc Adv.* 5, 1852–1858. doi: 10.1039/C4RA10767E
- Yuan, Y. J., Tu, J. R., Lu, H. W., Yu, Z. T., Fan, X. X., and Zou, Z. G. (2016). Neutral nickel(II) phthalocyanine as a stable catalyst for visible-light-driven hydrogen evolution from water. *Dalton Transact.* 45, 1359–1363. doi: 10.1039/C5DT04311E
- Yuan, Y. J., Yu, Z. T., Chen, D. Q., and Zou, Z. G. (2017). Metal-complex chromophores for solar hydrogen generation. *Chem. Soc. Rev.* 46, 603–631. doi: 10.1039/C6CS00436A
- Zee, D. Z., Chantarojsiri, T., Long, J. R., and Chang, C. J. (2015). Metal-polypyridyl catalysts for electro- and photochemical reduction of water to hydrogen. *Acc. Chem. Res.* 48, 2027–2036. doi: 10.1021/acs.accounts.5b00082

Conflict of Interest Statement: The authors declare that the research was conducted in the absence of any commercial or financial relationships that could be construed as a potential conflict of interest.

Copyright © 2019 Panagiotakis, Landrou, Nikolaou, Putri, Hardré, Massin, Charalambidis, Coutsolelos and Orio. This is an open-access article distributed under the terms of the Creative Commons Attribution License (CC BY). The use, distribution or reproduction in other forums is permitted, provided the original author(s) and the copyright owner(s) are credited and that the original publication in this journal is cited, in accordance with accepted academic practice. No use, distribution or reproduction is permitted which does not comply with these terms.